

Detection and Concealment of Transmission Errors in MPEG-4 Images*

CHIEN-MING LEE AND JIN-JANG LEOU

*Department of Computer Science and Information Engineering
National Chung Cheng University
Chiayi, 621 Taiwan*

For entropy-coded MPEG-4 images, a transmission error in a codeword may cause the underlying codeword and its subsequent codewords within a video packet to be misinterpreted, resulting in great degradation of the received MPEG-4 images. Here a transmission error may be a single-bit error or a burst error. In this study, a postprocessing approach to detection and concealment of transmission errors in MPEG-4 images is proposed. In this study, transmission errors within a video packet of an MPEG-4 image bitstream are detected by means of two successive procedures: (1) whether the video packet is corrupted or not is determined by checking a set of error-checking conditions, and then (2) the precise location (block-based) of the first transmission error (the first corrupted block) within the corrupted video packet is verified by using a backtracking procedure. To recover the corrupted shape data, the error concealment approach to the shape data of intra-coded IVOPs proposed in [4] is adopted, and an error concealment approach to the shape data of inter-coded P- and BVOPs is proposed in this study. To recover the corrupted texture data, several existing and proposed concealment techniques are employed together to generate a set of possible concealment candidates for a corrupted texture block. Then, an objective cost function is proposed here to determine the "best" texture error concealment candidate among the set of generated candidates as the concealed texture block for the corrupted texture block. Based on the simulation results obtained in this study, the proposed approach can recover high-quality MPEG-4 images from the corresponding corrupted MPEG-4 images. This shows the feasibility of the proposed approach.

Keywords: transmission error, MPEG-4 image, error detection, error concealment, shape data, texture data

1. INTRODUCTION

For entropy-coded MPEG-4 images [1], a transmission error in a codeword may cause the underlying codeword and its subsequent codewords to be misinterpreted, resulting in great degradation of the received images. To limit the propagation effect of transmission errors, MPEG-4 inserts synchronization codewords into the compressed bitstream. After the decoder receives a synchronization codeword, it resynchronizes the decoding operation regardless of the preceding slippage or transmission errors. Although the propagation effect of transmission errors can be terminated when a synchronization

Received August 27, 2001; revised March 6, 2003; accepted May 12, 2003.

Communicated by Ja-Ling Wu.

* This work was supported in part by National Science Council, R.O.C. under Grants NSC 90-2213-E-194-044 and NSC 91-2213-E-194-025.

codeword is correctly received, a transmission error will affect the underlying codeword and its subsequent codewords within a corrupted video packet, and will greatly degrade the quality of the received MPEG-4 images, as an illustrated example shown in Fig. 1. Note that the section between two successive synchronization codewords is called a video packet. Several error concealment techniques to eliminate the visual effect induced by transmission errors within H.261, H.263, MPEG-1, MPEG-2, and MPEG-4 images have been proposed [2]. However, within most error concealment methods, it is assumed that transmission errors are either detected or known. Additionally, these methods lack in a good objective cost function for error concealment. In this study, a postprocessing approach to detection and concealment of transmission errors in MPEG-4 images is proposed.

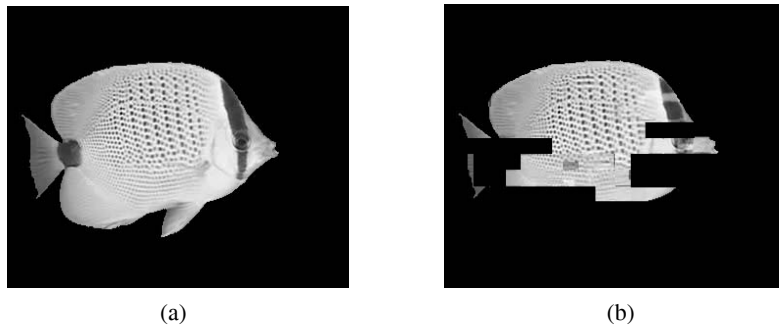


Fig. 1. The original and corrupted MPEG-4 images of the 9th VOP of the “Bream” sequence with a bit error rate = 0.05%: (a) the original image; (b) the corrupted image.

There are several approaches to concealing corrupted shape data in MPEG-4 images. Frater et al. [3] used the motion vectors of the spatially or temporally neighboring macroblocks to estimate the missing motion vectors. The missing texture is then replaced with the previous VOP using the recovered motion vector. Shirani, Erol, and Kossentini [4] proposed a Maximum a Posteriori (MAP) estimator to recover the missing shape data in IVOP. The statistical method is used to estimate the most likely shape data. Lee et al. [5] proposed an error concealment algorithm based on fuzzy set theory to repair damaged portions of the shape information.

There are four main strategies for eliminating the image quality degradation effect induced by transmission errors, including (1) the channel coding strategy, (2) the error resilient (preprocessing) strategy, (3) the encoder-decoder interactive error control strategy, and (4) the error concealment (postprocessing) strategy. The error resilient (preprocessing) strategy can be further divided into 6 categories, namely, (1) the resynchronization approach, (2) the robust entropy coding and prediction approach, (3) the layer coding with unequal error protection approach, (4) the multiple description coding approach, (5) the data partitioning approach, and (6) the RVLCs (reversible variable length codes) approach. In the channel coding approach, some error correcting codes are used to encode images such that transmission errors can be detected and corrected by using additional side information [6, 7]. Although the channel coding approach can detect and/or

correct transmission errors to a small extent, it moderately increases the transmission bit rate. Moreover, if the transmission errors exceed the error-correcting capability of an error correcting code, then the receiver will still fail to correctly decode the corrupted image bitstream.

In the error resilient (preprocessing) strategy, some preprocessing steps are performed at the encoder, i.e., the encoder is usually modified in some way [1, 8-14, 38, 39]. Usually, this will increase the transmission bit rate. In the resynchronization approach [1, 8], resynchronization markers are inserted into the compressed image/video bitstream at various locations. When the decoder detects an error, it can then hunt for a resynchronization marker and regain resynchronization. In the robust entropy coding and prediction approach, a technique called error-resilient entropy coding (EREC), developed by Redmill and Kingsbury [9], divides the whole bitstream into blocks of variable-length coded data and then reorganizes the compressed data such that each block starts at a known position within the bitstream. Several error resilient prediction approaches [10] limited temporal error propagation by inserting intra-coded frames or macroblocks. Because too many intra-coded frames or macroblocks will increase the bit rate, the coding mode (intra or inter) of each frame or macroblock must be determined carefully so as to optimize the tradeoff between compression efficiency and error resilience. In the layered coding with unequal error protection approach [11], an image/video bitstream is divided into a base layer and one or several enhancement layer(s). The base layer contains the more important information, such as the header and motion information, and provides lower but acceptable image/video quality, whereas the enhancement layer(s) contains the remaining information and incrementally improves the image/video quality. The base layer and enhancement layer(s) must be protected by means of unequal error protection, in which the base layer is protected more strongly. The multiple description coding approach [12] divides an image/video bitstream into several sub-bitstreams, known as descriptions. In contrast to the layer coding approach, the relationship between the descriptions is nonhierarchical and correlated, and the descriptions have similar importances. Any single description can provide basic quality, and more descriptions together will provide improved quality. In the data partitioning approach [8, 13, 14], the encoding data, such as the shape, motion, and texture data, are separated (partitioned) by shape and/or motion marker(s) so that the compressed image/video bitstream can guarantee error resilient transmission with small overhead (induced by shape and/or motion marker(s)). If the decoder detects an error, it loses synchronization and, hence, typically has to discard all the data up to the next resynchronization point. RVLCs are special VLCs that have the prefix property when decoding is done in both the forward and reverse directions [8, 38, 39]. By using RVLCs, the decoder can recover some of the compressed data that would otherwise have been discarded with small loss of compression efficiency.

In the encoder-decoder interactive error control strategy, a feedback channel can be set up from the decoder to the encoder [15]. The decoder can inform the encoder about which parts of the transmitted information are corrupted (due to transmission errors), and then the encoder can adjust its encoding operations accordingly to suppress or eliminate the effect of transmission errors. If the automatic repeat request (ARQ) function is supported, the corrupted (lost) packets can be retransmitted. But this approach is not suitable for real-time applications due to processing delays.

In the error concealment (postprocessing) strategy [16-36], based on the redundancy information inherent in neighboring pixels, the constraints on compressed image/video data, and the accompanying statistical property changes of received pixels owing to transmission errors, transmission errors can be directly detected and then corrected [16, 17] or concealed [18-36] without changing the encoder or embedding redundant bits. Error concealment techniques can be generally divided into three categories, namely, (1) spatial/spectral error concealment methods, (2) temporal error concealment methods, and (3) hybrid error concealment methods. In the spatial (or spectral) error concealment methods, the information received from the correctly reconstructed blocks and/or the previously concealed blocks spatially neighboring to a corrupted block is used to conceal the corrupted block [18-26]. The spatial/spectral error concealment approach works well only on smooth or regular image blocks. For irregular image blocks, it will produce undesired blurred image blocks. In temporal concealment methods, the information of the corresponding blocks and/or their neighboring blocks from the previous/successive frames of a corrupted block is used to conceal the corrupted block [27-30]. The temporal error concealment methods do not work well when the motion vector differences between the corrupted block and its neighboring blocks are too large, i.e., when the video sequence contains many unsmoothed moving blocks. For hybrid error concealment methods, all the information in spatial, spectral, and temporal domains is employed to conceal the corrupted blocks [31-36].

Each of the above-mentioned error concealment methods has its own weakness. Some of them made the assumption that each corrupted block is determined or known, whereas some of them are computationally expensive [18]. Additionally, they lack in a good cost function for error concealment. In this study, a postprocessing approach to detection and concealment of transmission errors in MPEG-4 images is addressed. The objective is to detect and conceal transmission errors in MPEG-4 images, i.e., to recover high quality MPEG-4 images from the corresponding corrupted image without increasing the transmission bit rate. Transmission errors within a video packet are detected by using two successive procedures: (1) whether the video packet is corrupted or not is detected by checking a set of error-checking conditions under decoding, and then (2) the precise location (block-based) of the first transmission error (the first corrupted block) within the video packet is verified by using a backtracking procedure.

After all the corrupted blocks within a corrupted video packet are detected by the proposed error detection approach, to recover (conceal) the corrupted shape data, the error concealment approach to the shape data of intra-coded IVOPs developed in [4] is adopted and an error concealment approach to the shape data of inter-coded P- and BVOPs is proposed in this study. To recover (conceal) the corrupted texture data, several existing and proposed concealment techniques using spatial and temporal information are employed together to generate a set of possible concealment candidates for each corrupted texture block. Then an objective cost function for texture error concealment is proposed here to determine the "best" texture error concealment candidate among the set of generated candidates as the concealed texture block for the corrupted texture block.

In this study, a transmission error may be a single-bit error or a burst error. However, to simplify the processing steps in the proposed approach, a burst error containing several error bit segments will be treated as several transmission errors, i.e., a transmission error is equivalent either a single-bit error or a burst error containing N successive error

bits. And for simplicity, it is assumed that: (1) the VOL, VO, and VOP codewords and their headers are correctly received; (2) each header followed a resynchronization code-word is correctly received.

The paper is organized as follows. The proposed postprocessing approach to detection and concealment of transmission errors in MPEG-4 images is addressed in section 2. Simulation results are included in section 3, followed by concluding remarks.

2. DETECTION AND CONCEALMENT OF TRANSMISSION ERRORS IN MPEG-4 IMAGES

The procedure for decoding an MPEG-4 compressed bitstream can be translated into the flowchart shown in Fig. 2. The proposed error detection and concealment approach is embedded in the modified Decode_VOP procedure shown in Fig. 3. The goal of the start code determination procedure is to find the video packet start code (VPSC) of the current VOP. Within a VOP, after these start codes are determined, i.e., after each video packet (the minimum synchronization unit) within the VOP is identified, the proposed error detection approach is performed on the video packet within the VOP sequentially so that all the corrupted blocks in the VOP can be detected. After all the corrupted blocks are determined by the proposed error detection approach, the proposed error concealment approach is employed to conceal all the corrupted blocks in the VOP.

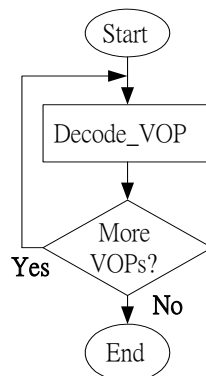


Fig. 2. The procedure for decoding an MPEG-4 compressed bitstream.

2.1 Proposed Error Detection Approach

Within the start code determination procedure, the Seek_VSC procedure is used first to find the VOP start code (VSC) of the current VOP, and the Seek_VPSC procedure is then used repeatedly to find the VPSCs within the VOP. Because the number of video packets within a VOP is not fixed, the algorithm is used repeatedly until the next VSC is found.

After the start code determination procedure has been performed on a VOP, i.e., after all the VPSCs have been determined, the decoder decodes each video packet within

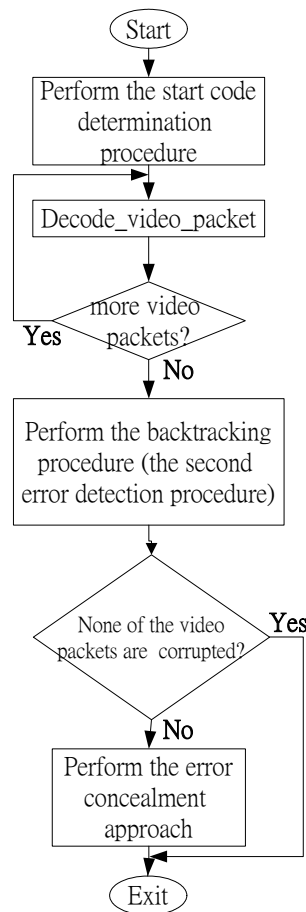


Fig. 3. The modified Decode_VOP procedure.

the VOP. Transmission errors within each video packet of a VOP are detected by means of two successive procedures [35]: (1) whether a video packet is corrupted or not is determined by checking a set of error-checking conditions, and then (2) the precise location (block-based) of the first transmission error within a corrupted video packet is verified by using a backtracking procedure. The first procedure of the proposed error detection approach is included within the Decode_video_packet procedure.

The error-checking conditions for the proposed error detection approach are derived from the constraints imposed on MPEG-4 video bitstream syntax, which are listed as follows.

- (1) An invalid codeword for the Huffman code, DCT coefficient, motion vector code, MCBPC code, CBPY, DQUANT, MBTYPE code, or shape mode code is found.
- (2) The total number of decoded macroblocks in a video packet is not equal to the size identified by the two successive video packet headers.

- (3) The number of decoded DCT coefficients within a block is larger than 64.
- (4) Physically impossible image data are detected. For example, the prediction error between the predicted block and the current block is out of range.

If any of the above error-checking conditions is satisfied, we stop decoding the current video packet, mark the current block and its subsequent blocks within the current video packet as corrupted blocks, and mark the current video packet as a corrupted video packet.

The first error detection procedure preliminarily determines whether the current video packet is corrupted or not. The position (block-based) of the first transmission error of a video packet usually can not be precisely determined by the first error detection procedure. As shown in Fig. 4, the second procedure of the proposed error detection approach is used to determine the “true” first corrupted block within a corrupted video packet by backtracking from the corrupted macroblock containing the first corrupted block detected by the first error detection procedure.

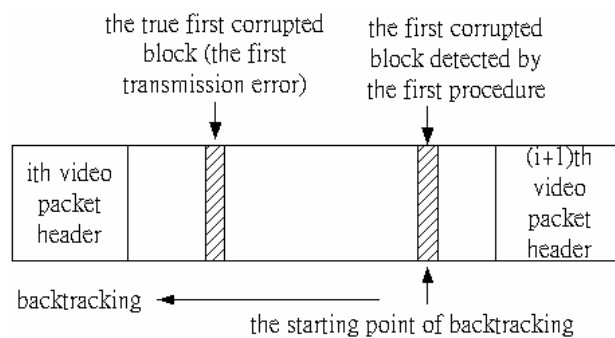


Fig. 4. The second procedure of the proposed error detection approach with block-based backtracking.

In general, the average intersample difference of a corrupted block will be relatively larger than that of the corresponding correctly-decoded block or that of a correctly-decoded neighboring block. First, based on the above observation, a measure employed by Han and Leou [17], namely, the average intersample difference (AID) of a block C ($N \times M$ in size), is first employed in this study to check whether a block is corrupted or not. *AID* is given by

$$AID(C) = \frac{\sum_{y=0}^{N-1} \sum_{x=1}^{M-1} |C(x, y) - C(x-1, y)| + \sum_{x=0}^{M-1} \sum_{y=1}^{N-1} |C(x, y) - C(x, y-1)|}{N \times (M-1) + M \times (N-1)}, \tag{1}$$

where $C(x, y)$ is the pixel value of position (x, y) within block C (using a local coordinate system).

Second, it is intuitively known that the block boundaries between a correctly-received block and its 4-connected “believable” neighboring blocks will be very smooth. Note that a correctly received block or a concealed block is a “believable” block. Another measure, namely, the average intersample difference of the block boundary (*AIDB*) between block C and all the believable neighboring blocks is defined as [35]

$$AIDB(C) = \frac{1}{|BN_C \cap N_C|} \sum_{B_i \in BN_C \cap N_C} ABD(C, B_i), \quad (2)$$

where $|X|$ denotes the total number of blocks within the set X , BN_C is the set containing all the believable neighboring blocks of block C , N_C is the set containing all the 4-connected neighboring blocks of block C , and

$$ABD(C, X) = \begin{cases} \frac{1}{8} \sum_{i=0}^7 |C(0, i) - X(7, i)|, & \text{if } X \text{ is the above neighboring block of } C, \\ \frac{1}{8} \sum_{i=0}^7 |C(7, i) - X(0, i)|, & \text{if } X \text{ is the below neighboring block of } C, \\ \frac{1}{8} \sum_{i=0}^7 |C(i, 0) - X(i, 7)|, & \text{if } X \text{ is the left neighboring block of } C, \\ \frac{1}{8} \sum_{i=0}^7 |C(i, 7) - X(i, 0)|, & \text{if } X \text{ is the right neighboring block of } C. \end{cases} \quad (3)$$

AIDB(C) is also employed in this study to check whether a block is corrupted or not.

Third, it can be observed that the textures of a block and its 4-connected or 8-connected neighboring blocks within an image are usually similar. Several statistical measures for evaluating the characteristic differences between a block and its 4-connected believable neighboring blocks, namely, the average AID difference (*AAIDD*), the average mean difference (*AMD*), and the average variance difference (*AVD*) are defined as follows:

$$AAIDD(C) = \frac{1}{|BN_C|} \sum_{B_i \in BN_C} |AID(C) - AID(B_i)|, \quad (4)$$

$$AMD(C) = \frac{1}{|BN_C|} \sum_{B_i \in BN_C} |Mean(C) - Mean(B_i)|, \quad (5)$$

$$AVD(C) = \frac{1}{|BN_C|} \sum_{B_i \in BN_C} |Variance(C) - Variance(B_i)|. \quad (6)$$

For the above five measures, five corresponding thresholds, namely, Th_{AID} , Th_{AIDB} , Th_{AAIDD} , Th_{AMD} , and Th_{AVD} , are set by means of the statistics of several training image sequences. If any of the five measures of a block is larger than the corresponding thresh-

old, the block will be determined as a corrupted block. And if any block of a macroblock is corrupted, the macroblock is determined as a corrupted one.

2.2 Proposed Error Concealment Approach

2.2.1 Proposed error concealment approach for shape data

According to the types of VOPs (I-, P-, and BVOPs), block-wise shape data are either intra- or inter-coded. In this study, the error concealment approach to the shape data of intra-coded IVOPs described in [4] is employed, and an error concealment approach to the shape data of inter-coded P- and BVOPs is proposed here.

A. Concealment of the shape data of intra-coded IVOPs

In [4], it was noted that the binary pixel values in an image or video signal are realizations of an underlying statistical model. The Bayesian approach provides *a priori* information by selecting the image model. Then, if the observed image data are given, the Maximum a Posteriori (MAP) estimation yields the most likely image.

The MAP estimation of the missing shape data of an image, which assumes that MRF is the image *a priori* model, can be expressed as

$$\hat{X} = \min_{x_{i,j}} \sum_{i,j \in M} V(x_{i,j}), \quad (7)$$

where M is the set of all missing binary pixels in the image and V is the potential function. The potential function characterizes the relationship between a group of binary pixels by assigning larger costs to the binary pixels that are less likely to occur. The potential function is selected as [4]

$$\sum_{c \in C_c} V(x_{i,j}) = \sum_{k,l \in c} w_{i,j \rightarrow k,l} \rho(x_{i,j} - x_{k,l}), \quad (8)$$

where c is the clique, C_c is the set of all cliques throughout the image, ρ is the cost function, and $w_{i,j \rightarrow k,l}$ is the weight assigned to the difference between the pixel values $x_{i,j}$ and $x_{k,l}$. The cost function $\rho(\cdot)$, encouraging the pixels that are spatially close to each other to have the same values, is defined as

$$\rho(x) = \begin{cases} \beta, & x \neq 0, \\ 0, & x = 0, \end{cases} \quad (9)$$

where β is a positive constant. For the clique, an eight-pixel neighborhood is selected and shown in Fig. 5.

The weight corresponding to the difference between a binary pixel and one of the binary pixels in its clique is selected based on the likelihood of an edge occurring in the direction of the subject pair of binary pixels. The rationale behind this selection is to give

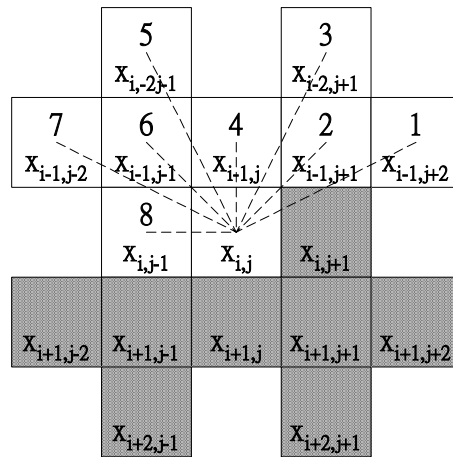


Fig. 5. A corrupted pixel $x_{i,j}$, its clique (from pixels 1 to 8), and the eight directions. The complement of the clique is the shaded area.

greater weight to the difference between the binary pixels in a direction which will cause the values of the binary pixels in that direction to be the same. Assuming that the values $w_{i,j \rightarrow k,l}$ are integers, the estimated value of a binary pixel given the values of the binary pixels in its clique is defined as [4]

$$\begin{aligned}
 \hat{x}_{i,j} &= \min_{x_{i,j}} \sum_{(k,l) \in c \cup c'} w_{i,j \rightarrow k,l} \rho(x_{i,j} - x_{k,l}) \\
 &= \min \left[\underbrace{\rho(x_{i,j} - x_{i,j+1}) + \dots + \rho(x_{i,j} - x_{i,j+1})}_{w_{i,j \rightarrow i,j+1} \text{ times}} \right. \\
 &\quad \left. + \dots + \underbrace{\rho(x_{i,j} - x_{i+1,j+2}) + \dots + \rho(x_{i,j} - x_{i+1,j+2})}_{w_{i,j \rightarrow i+1,j+2} \text{ times}} \right], \tag{10}
 \end{aligned}$$

where c' is the complement of the clique shown in Fig. 5. To minimize the value of the potential function, the number of terms with an estimated value that is different from that of the neighboring binary pixel should be minimized. Therefore, the estimated value should be equal to the median of the following vectors:

$$\hat{x}_{i,j} = \text{median} \left[\underbrace{x_{i,j+1}, \dots, x_{i,j+1}}_{w_{i,j \rightarrow i,j+1} \text{ times}}, \dots, \underbrace{x_{i+1,j+2}, \dots, x_{i+1,j+2}}_{w_{i,j \rightarrow i+1,j+2} \text{ times}} \right]. \tag{11}$$

The likelihood of edges occurring in each of the eight directions is computed using shape blocks around the corrupted shape block. In this study, the available shape information in the believable neighboring shape blocks (4-connected) of the corrupted shape block is exploited in the concealment process. First, a pixel is declared inside the shape if

all the four neighboring pixels (above, below, left, and right) of the pixel are inside the shape. Otherwise, the pixel is assigned to the border of the shape. A 3×3 window centered at each border pixel and the angle of the best line-fit to the border pixels in the window are computed. This gives the direction of the edge at the pixel in the center of the window. The counter corresponding to the direction of the detected edge (best line-fit) is incremented if the extension of the best line-fit passes through the corrupted block. The procedure is repeated for all the border pixels in the blocks to the right, left, below, and above the corrupted block (if believable). The weights required in the estimation function are defined as [4]

$$w_{i,j \rightarrow k,l} = c_m, \quad (12)$$

where c_m is the counter corresponding to direction m , which corresponds to the direction formed by (i, j) and (k, l) . Finally, the proposed error concealment method for the shape data of IVOPs can be summarized as follows.

- Step 1:** Determine the edges in the neighboring blocks and assign them to eight equally spaced directions. Compute the corresponding counter for each direction.
- Step 2:** Find a set of weights for each corrupted block using counters obtained in Step 1.
- Step 3:** Use the estimation function to obtain an estimate of each corrupted pixel using the weights obtained in Step 2.
- Step 4:** Iteratively re-estimate the missing pixels using Step 3 until convergence achieved.

The reconstruction algorithm is applied recursively. Blocks with the maximum number of correctly decoded neighboring blocks are reconstructed first, and the rest of the blocks are reconstructed recursively.

B. Concealment of the shape data of P- and BVOPs

For a corrupted shape block of a P- or BVOP, a set of candidates for a corrupted shape block, SC , is first generated, and then a proposed smooth function for shape error concealment (or shape recovery) is used to select the “best” candidate among SC as the concealed shape block for the corrupted shape block of P- and BVOPs.

The set of candidates for a corrupted shape block, SC , includes the following types of candidate shape blocks.

- (1) The corresponding shape block (in the reference VOP) of the corrupted shape block.
- (2) All the “believable” neighboring shape blocks of the corrupted shape block.
- (3) All the motion-compensated shape blocks (in the reference VOP) with their motion vectors being the motion vectors of all the “believable” neighboring shape blocks of the corrupted shape block.
- (4) All the motion-compensated shape blocks (in the reference VOP) with their motion vectors being the motion vectors of all the “believable” neighboring blocks of the corrupted shape block.

In general, the boundaries between the concealed shape block and its believable neighboring shape blocks will be very smooth. Therefore, the boundary difference $BDS(C, X)$ between a concealed shape block (candidate) C and its believable neighboring shape block X is defined as

$$BDS(C, X) = \begin{cases} \sum_{j=0}^7 |C(0, j) - X(7, j)|, & \text{if } X \text{ is the above believable neighboring block of } C, \\ \sum_{j=0}^7 |C(7, j) - X(0, j)|, & \text{if } X \text{ is the below believable neighboring block of } C, \\ \sum_{i=0}^7 |C(i, 0) - X(i, 7)|, & \text{if } X \text{ is the left believable neighboring block of } C, \\ \sum_{i=0}^7 |C(i, 7) - X(i, 0)|, & \text{if } X \text{ is the right believable neighboring block of } C, \end{cases} \quad (13)$$

where $C(i, j)$ and $X(i, j)$ denote the pixel values of position (i, j) within shape blocks C and X , respectively. Exploiting the $BDS(C, X)$ measure, the smooth function for shape error concealment $SF(C)$ of a concealed shape block (candidate) C is defined as

$$SF(C) = \sum_{B_i \in BN_C \cap N_C} BDS(C, B_i). \quad (14)$$

In the proposed approach, a candidate C with the minimum “mismatch” pixels obtained by $SF(C)$ is preferred because it is the smoothest in the boundary between the candidate and the believable neighboring shape blocks of the corrupted shape block.

2.2.2 Proposed error concealment approach for texture data

In this study, a set of candidates for a corrupted texture block, SC , is first generated, and then a proposed cost function for texture error concealment is used to select the “best” candidate among SC as the concealed texture block for the corrupted texture block.

The set of candidates for a corrupted texture block, SC , includes all the following types of candidate texture blocks [35].

- (1) All the believable neighboring texture blocks of the corrupted texture block.
- (2) The “average” block of all the believable neighboring texture blocks of the corrupted texture block.
- (3) The “median” block of all the believable neighboring texture blocks of the corrupted texture block.
- (4) All the motion-compensated blocks (in the reference VOP) with their motion vectors being the motion vectors of all the believable neighboring texture blocks of the corrupted texture block.
- (5) The motion-compensated block (in the reference VOP) with its motion vector being

the “average” of the motion vectors of all the believable neighboring texture blocks of the corrupted texture block.

- (6) The motion-compensated block (in the reference VOP) with its motion vector being the “median” of the motion vectors of all the believable neighboring texture blocks of the corrupted texture block.
- (7) The “average” block of the motion-compensated blocks (in the reference VOP) of all the believable neighboring texture blocks of the corrupted texture block.
- (8) The “median” block of the motion compensated blocks (in the reference VOP) of all the believable neighboring texture blocks of the corrupted texture block.

In general, a concealed texture block usually has statistical/spectral/spatial properties similar to those of its believable neighboring texture blocks. The boundaries between the concealed texture block and its believable neighboring texture blocks will be very smooth. First, the proposed fitness function, CF , will include $AIDB$ for evaluating the smoothness of the boundaries. Second, to take advantage of statistical mean and variance, the proposed fitness function will include two measures, AMD and AVD , between a concealed texture block (candidate) and its believable neighboring texture blocks. Third, in terms of temporal correlation, a corrupted texture block usually has a motion vector similar to those of its believable neighboring texture blocks. Thus, a corrupted texture block will be very similar to the motion-compensated texture block in the reference VOP. The shadow block S of a corrupted texture block is defined as the motion-compensated texture block in the reference VOP with the motion vector being the “average” or the “median” of the motion vectors of the believable neighboring texture blocks of the corrupted texture block. Based on simulation results obtained in this study, the “average” motion vector is employed. Based on shadow block S , the shadow difference $SD(C, S)$ between a concealed texture block (candidate) C and its shadow block S is defined as

$$SD(C, S) = \frac{1}{64} \sum_{i=0}^7 \sum_{j=0}^7 |C(i, j) - S(i, j)|, \quad (15)$$

where $C(i, j)$ and $S(i, j)$ denote the pixel values of blocks C and S , respectively.

Combining the above four measures, $AIDB$, AMD , AVD , and SD , the proposed cost function for texture error concealment, $CF(C)$, of a concealed texture block (candidate) C is defined as

$$CF(C) = W_S \times SD(C, S) + W_B \times AIDB(C) + W_M \times AMD(C) + W_V \times AVD(C), \quad (16)$$

where W_S , W_B , W_M , and W_V are weighting coefficients, which are adjusted adaptively by the spatial relationship and the number of believable neighboring texture blocks for the corrupted texture block. In particular, the total number of believable neighboring texture blocks, N , and the total number of believable neighboring texture blocks which are correctly-received or temporally-concealed, N_V , are used to adjust W_S adaptively. Additionally, information about whether the believable neighboring texture blocks of a corrupted texture block C are uniform (or smooth) blocks or not can be used to adjust W_B , W_M , and W_V . The weighting coefficient assignments for different cases are summarized in Table 1.

Table 1. The weighting coefficient assignments for different cases.

		Uniform				Not Uniform			
		W_S	W_B	W_M	W_V	W_S	W_B	W_M	W_V
$N_V = 0$	First VOP	0	0.34	0.33	0.33	0	0.66	0.17	0.17
	Nonfirst VOP	0.1	0.3	0.3	0.3	0.1	0.6	0.15	0.15
$N_V < N/2$		0.52	0.16	0.16	0.16	0.52	0.32	0.08	0.08
$N_V \geq N/2$		0.79	0.07	0.07	0.07	0.79	0.13	0.04	0.04

3. SIMULATION RESULTS

Three MPEG-4 test video sequences, “Bream,” “Coastguard,” and “Weather,” with different bit error rates (BER) and different average lengths of burst errors (N_{ave}) are used to evaluate the performance of the proposed approach. For the three testing sequences, each sequence consists of 30 video frames, a GOV (group of VOPs) consists of 9 VOPs ($N = 9$), and the number of BVOPs between I- or PVOPs is 2 ($M = 3$). The average length of burst errors N_{ave} is given by

$$N_{ave} = \sum_{i=1}^N iP_i, \quad (17)$$

where P_i is the probability of a burst error containing i successive error bits with $\sum_{i=1}^N P_i = 1$. In this study, N (the maximum number of successive error bits of a burst error) is set to 5, but it can be set to a larger number without any difficulty.

The peak signal to noise ratio ($PSNR$) is employed in this study as the objective performance measure for the three components (Y, U, and V) of MPEG-4 images. The $PSNR$ of the i th VOP in an MPEG-4 video sequence, denoted by $PSNR_i$, is defined as

$$PSNR_i = (4 \times PSNR_{Y,i} + PSNR_{U,i} + PSNR_{V,i})/6, \quad (18)$$

where $PSNR_{Y,i}$, $PSNR_{U,i}$, and $PSNR_{V,i}$ are the corresponding $PSNR$ values of the Y, U, and V components of the i th VOP, respectively. The average $PSNR$ of an MPEG video sequence, denoted by $PSNR_{seq}$, is given by

$$PSNR_{seq} = \sum_{i=1}^n (PSNR_i) / n, \quad (19)$$

where n is the total number of VOPs in the MPEG-4 video sequence.

To determine the thresholds used in this study, the statistical distributions of AID , $AIDB$, $AAIDD$, AMD , and AVD for the three test sequences are calculated in advance. Based on the statistical distributions obtained in this study, the threshold Th_{AID} for AID is set to 50 for the Y component and 20 for both the U and V components. The threshold Th_{AIDB} for $AIDB$ is set to 65 for the Y component and 30 for both the U and V compo-

nents. The threshold Th_{AAIDD} for *AAIDD* is set to 50 for the Y component and 15 for both the U and V components. The threshold Th_{AMD} for *AMD* is set to 70 for the Y component and 30 for both the U and V components. The threshold Th_{AVD} for *AVD* is set to 5000 for the Y component and 1300 for both the U and V components. The thresholds Th_{MD} and Th_{VD} used to determine whether the believable neighboring blocks are uniform or not are set to 49 and 1305, respectively.

The similarity between an error-concealed shape data and its original shape data is given by

$$\eta = 1 - \frac{n_d}{n_t}, \quad (20)$$

where n_d is the number of pixels that are different between the error-concealed shape and the original one, and n_t is the total number of pixels in the boundary box. Table 2 lists the ratio for the three test sequences using the proposed shape recovery approach. The simulation results without/with shape recovery with $BER = 0.05\%$ and $N_{ave} = 4$ for the two test sequences, “Bream” and “Weather,” are shown in Figs. 6-7, respectively.



Fig. 6. The simulation results without (a) and with (b) application of the proposed shape recovery approach to the 8th VOP of the “Bream” sequence with $BER = 0.05\%$ and $N_{ave} = 4$.



Fig. 7. The simulation results without (a) and with (b) application of the proposed shape recovery approach to the 9th VOP of the “Weather” sequence with $BER = 0.05\%$ and $N_{ave} = 4$.

Table 2. The simulation results, the similarity η , of shape data for the “Bream,” “Coastguard,” and “Weather” sequences, under different values of BER and N_{ave} , obtained using the proposed shape recovery approach.

BER	N_{ave}	Bream	Coastguard	Weather
0.01%	1	0.9995	0.9979	0.9992
	2	0.9993	0.9903	0.9998
	3	0.9997	0.9958	0.9998
	4	0.9950	0.9964	0.9997
	5	0.9983	0.9979	0.9996
0.03%	1	0.9946	0.9957	0.9992
	2	0.9944	0.9948	0.9991
	3	0.9927	0.9837	0.9989
	4	0.9905	0.9918	0.9992
	5	0.9949	0.9933	0.9980
0.05%	1	0.9927	0.9821	0.9984
	2	0.9896	0.9883	0.9975
	3	0.9880	0.9947	0.9980
	4	0.9908	0.9880	0.9975
	5	0.9910	0.9904	0.9984
0.07%	1	0.9982	0.9887	0.9983
	2	0.9917	0.9934	0.9983
	3	0.9808	0.9718	0.9979
	4	0.9891	0.9912	0.9948
	5	0.9892	0.9745	0.9982
0.09%	1	0.9874	0.9857	0.9982
	2	0.9899	0.9810	0.9936
	3	0.9863	0.9874	0.9975
	4	0.9871	0.9878	0.9946
	5	0.9885	0.9856	0.9964
0.1%	1	0.9835	0.9866	0.9981
	2	0.9853	0.9849	0.9975
	3	0.9898	0.9892	0.9922
	4	0.9850	0.9757	0.9963
	5	0.9884	0.9843	0.9922
0.2%	1	0.9665	0.9780	0.9800
	2	0.9605	0.9695	0.9930
	3	0.9656	0.9841	0.9949
	4	0.9752	0.9632	0.9809
	5	0.9730	0.9589	0.9884
0.5%	1	0.9520	0.9491	0.9712
	2	0.9535	0.9383	0.9653
	3	0.9561	0.9257	0.9644
	4	0.9557	0.9437	0.9559
	5	0.9557	0.9227	0.9733

To compare the performances of existing error concealment approaches and the proposed approach for the texture data, four existing error concealment methods [22, 23, 32] are implemented in this study. The four existing error concealment methods include: (1) zero-substitution, which simply replaces all the pixels in a corrupted block by zeros, denoted as Zero-S; (2) spatial error concealment using multi-directional interpolation [22], denoted as Spatial-M; (3) spectral error concealment exploiting interblock correlation [23], denoted as Spatial-I; and (4) hybrid error concealment for the digital simulcast AD-HDTV decoder [32], denoted as Hybrid-A. In terms of $PSNR_{seq}$ in dB, a performance comparison between the four existing error concealment approaches, namely, Zero-S, Spatial-M, Spatial-I, and Hybrid-A, and the proposed approach (denoted by Proposed) for the two test video sequences, “Bream” and “Weather,” is given in Tables 3-4, respectively. As a subjective measure of the quality of the concealed images, the original and concealed MPEG-4 images (the Y component) obtained using the four existing error concealment approaches and the proposed approach with $BER = 0.05\%$ and $N_{ave} = 4$ for the two test video sequences, “Bream” and “Weather,” are shown in Figs. 8-9, respectively.

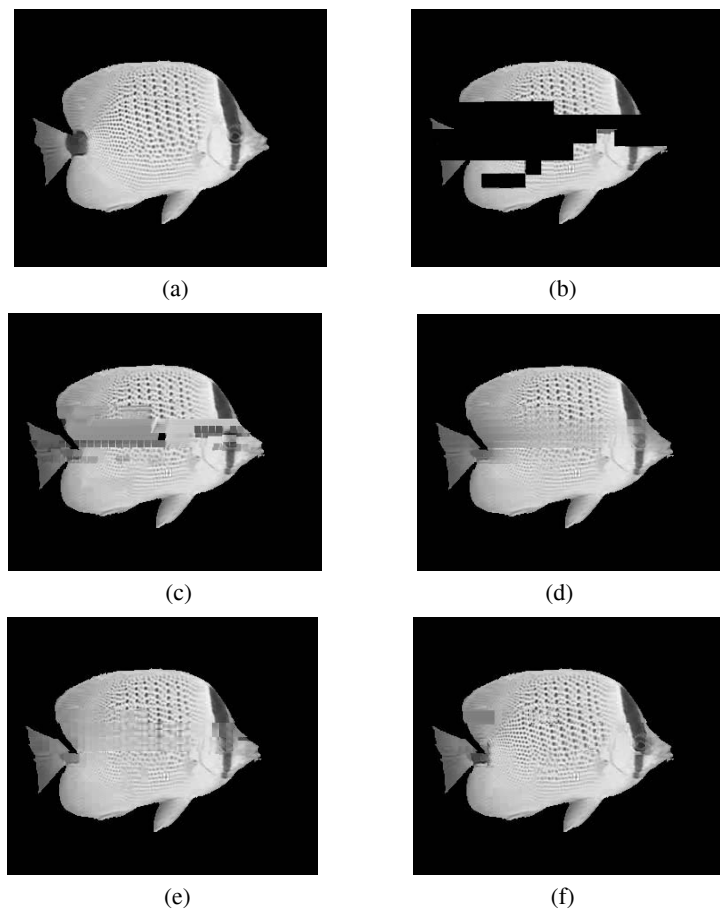


Fig. 8. The original and concealed MPEG-4 images (the Y component) of the 2nd VOP of the “Bream” sequence with $BER = 0.05\%$ and $N_{ave} = 4$: (a) the original VOP; (b)-(f) the concealed VOPs obtained using Zero-S, Spatial-M, Spectral-I, Hybrid-A, and the proposed approach, respectively.

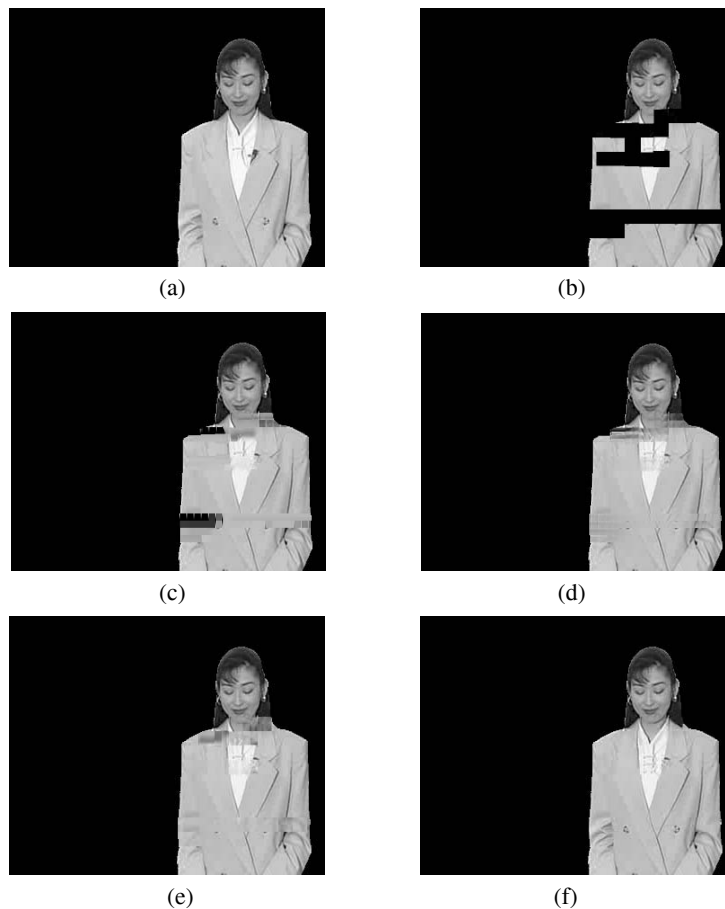


Fig. 9. The original and concealed MPEG-4 images (the Y component) of the 7th VOP of the “Weather” sequence with $BER = 0.05\%$ and $N_{ave} = 4$: (a) the original VOP; (b)-(f) the concealed VOPs obtained using Zero-S, Spatial-M, Spectral-I, Hybrid-A, and the proposed approach, respectively.

To illustrate the effectiveness of the proposed (hybrid) objective cost function for texture error concealment, which combines several error concealment performance measures from the spatial and temporal domains, a performance comparison of simulation results for the three test sequences obtained using the cost function $AIDB(C)$ and the proposed error concealment cost function $CF(C)$ is given in Table 5. To illustrate the effectiveness of the second (backtracking) procedure of the proposed error detection approach, a performance comparison of simulation results for the three test sequences obtained using the proposed detection and concealment approach without/with the second (backtracking) procedure is given in Table 6. The simulation results obtained using the proposed detection and concealment approach without/with the second (backtracking) procedure for the first VOP of the “Weather” sequence with $BER = 0.05\%$ and $N_{ave} = 4$ are shown in Fig. 10.

Table 3. The simulation results, $PSNR_{seq}$ in dB, for the “Bream” sequence, under different values of BER and N_{ave} , obtained using the four existing error concealment approaches and the proposed approach.

BER	N_{ave}	$PSNR_{seq}$ (dB)					
		Error-free	Zero-S	Spatial-M	Spectral-I	Hybrid-A	Proposed
0.01%	1	33.00	28.41	30.47	30.91	30.87	31.54
	2	33.00	24.46	30.21	30.66	30.39	31.36
	3	33.00	15.03	25.59	27.60	27.69	28.55
	4	33.00	16.40	24.80	26.24	26.06	27.21
	5	33.00	20.28	28.01	29.04	29.15	29.31
0.03%	1	33.00	13.50	22.55	25.26	24.27	25.98
	2	33.00	11.68	21.58	23.90	24.66	24.72
	3	33.00	14.90	24.29	25.65	25.52	26.63
	4	33.00	12.82	22.80	24.63	24.56	25.93
	5	33.00	14.90	22.74	25.50	24.80	25.59
0.05%	1	33.00	11.38	21.30	24.26	23.95	25.09
	2	33.00	13.09	22.57	24.55	23.78	25.40
	3	33.00	11.89	21.70	23.58	23.67	24.91
	4	33.00	12.22	23.01	25.22	24.78	26.16
	5	33.00	11.99	21.74	23.88	22.97	24.15
0.07%	1	33.00	10.77	19.83	22.39	21.46	23.30
	2	33.00	12.11	22.42	24.96	24.96	25.72
	3	33.00	9.64	18.92	21.72	21.03	22.53
	4	33.00	11.42	21.88	24.17	24.42	25.39
	5	33.00	10.70	20.92	23.68	23.35	24.61
0.09%	1	33.00	10.86	19.66	22.65	19.71	23.46
	2	33.00	10.45	20.05	23.23	23.13	24.02
	3	33.00	10.21	19.27	22.21	22.93	23.95
	4	33.00	9.72	20.52	23.17	22.45	24.28
	5	33.00	9.46	19.44	22.56	21.80	23.40
0.1%	1	33.00	10.89	20.48	23.03	22.93	24.12
	2	33.00	10.65	19.45	21.61	22.01	22.79
	3	33.00	9.86	19.50	22.61	21.69	23.60
	4	33.00	9.40	18.45	21.17	20.73	22.65
	5	33.00	10.00	20.40	23.20	22.63	23.87
0.2%	1	33.00	8.01	16.80	19.42	18.94	20.69
	2	33.00	7.14	16.40	19.54	18.23	20.37
	3	33.00	8.05	17.03	18.95	19.14	20.87
	4	33.00	7.82	15.76	18.52	19.09	20.42
	5	33.00	8.48	18.57	21.32	21.41	22.16
0.5%	1	33.00	6.18	15.86	17.74	16.87	19.46
	2	33.00	6.02	15.02	18.01	16.88	19.10
	3	33.00	6.19	15.10	18.25	17.51	18.99
	4	33.00	6.01	15.43	18.19	18.30	19.43
	5	33.00	5.42	15.03	17.96	17.26	19.08

Table 4. The simulation results, $PSNR_{seq}$ in dB, for the “Weather” sequence, under different values of BER and N_{ave} , obtained using the four existing error concealment approaches and the proposed approach.

BER	N_{ave}	$PSNR_{seq}$ (dB)					
		Error-free	Zero-S	Spatial-M	Spectral-I	Hybrid-A	Proposed
0.01%	1	34.67	18.80	27.43	28.54	28.25	29.19
	2	34.67	23.02	30.19	31.52	31.16	31.53
	3	34.67	19.84	30.35	30.43	30.32	30.55
	4	34.67	28.56	31.93	32.50	32.10	32.77
	5	34.67	27.99	31.42	31.63	31.59	32.16
0.03%	1	34.67	18.70	26.88	26.22	26.39	27.35
	2	34.67	18.56	29.36	28.86	27.78	29.67
	3	34.67	12.96	22.01	25.15	23.75	26.07
	4	34.67	15.26	23.19	26.04	24.68	27.38
	5	34.67	16.18	25.58	27.02	26.48	28.45
0.05%	1	34.67	10.89	18.84	21.39	18.49	22.56
	2	34.67	10.86	19.15	21.81	19.56	23.17
	3	34.67	11.26	20.40	23.34	21.85	24.13
	4	34.67	12.82	21.33	24.46	23.73	25.55
	5	34.67	11.36	19.70	23.26	20.48	23.38
0.07%	1	34.67	12.67	23.59	25.83	26.66	26.71
	2	34.67	11.62	21.05	26.03	25.67	26.77
	3	34.67	11.65	24.29	26.44	25.59	26.95
	4	34.67	10.27	17.85	19.33	18.81	21.15
	5	34.67	10.59	23.10	25.91	24.71	26.56
0.09%	1	34.67	10.96	21.68	22.93	22.55	23.46
	2	34.67	10.79	19.37	22.66	22.42	23.70
	3	34.67	10.18	19.38	22.69	23.98	24.38
	4	34.67	9.98	19.87	22.04	20.45	22.98
	5	34.67	9.85	19.52	21.48	20.84	22.67
0.1%	1	34.67	13.23	21.97	23.56	23.70	24.27
	2	34.67	11.49	21.28	23.81	22.01	24.25
	3	34.67	10.04	18.59	20.26	19.46	21.03
	4	34.67	9.94	18.67	22.45	20.53	22.83
	5	34.67	9.06	18.44	19.55	18.49	20.87
0.2%	1	34.67	7.92	17.53	19.45	17.99	20.48
	2	34.67	8.79	16.42	19.09	15.06	19.74
	3	34.67	9.14	16.58	19.30	16.97	19.34
	4	34.67	9.74	15.56	19.16	15.99	18.70
	5	34.67	7.82	15.94	17.63	15.37	18.53
0.5%	1	34.67	6.89	13.74	17.63	13.20	18.08
	2	34.67	6.74	13.70	17.82	13.76	19.05
	3	34.67	7.32	13.73	16.38	13.83	18.34
	4	34.67	6.71	13.92	15.61	12.49	17.16
	5	34.67	6.46	13.83	18.12	13.88	19.04

Table 5. The simulation results, $PSNR_{seq}$ in dB, for the “Bream,” “Coastguard,” and “Weather” sequences, under different values of BER and N_{ave} , obtained using the two different cost functions for error concealment, $AIDB(C)$ and $CF(C)$.

BER	N_{ave}	Bream		Coastguard		Weather	
		$AIDB(C)$	$CF(C)$	$AIDB(C)$	$CF(C)$	$AIDB(C)$	$CF(C)$
0.01%	1	27.79	31.54	32.73	36.37	27.68	29.19
	2	28.09	31.36	29.34	33.15	25.02	31.53
	3	23.83	28.55	30.19	35.30	26.94	30.55
	4	24.72	27.21	31.29	35.84	27.29	32.77
	5	25.12	29.31	32.23	36.14	28.51	32.16
0.03%	1	22.84	25.98	30.73	33.26	23.23	27.35
	2	20.78	24.72	29.26	34.30	25.56	29.67
	3	21.65	26.63	28.67	34.76	24.01	26.07
	4	21.36	25.93	27.05	30.91	23.00	27.38
	5	21.24	25.59	28.35	32.14	25.91	28.45
0.05%	1	22.13	25.09	27.47	30.77	20.64	22.56
	2	20.73	25.40	29.92	32.84	21.99	23.17
	3	21.55	24.91	31.79	34.38	20.71	24.13
	4	21.05	26.16	30.51	33.05	22.28	25.55
	5	20.48	24.15	27.35	31.20	21.08	23.38
0.07%	1	20.52	23.30	26.35	30.90	22.30	26.71
	2	22.15	25.72	28.77	31.64	23.34	26.77
	3	19.67	22.53	24.15	27.82	21.06	26.95
	4	23.01	25.39	26.45	31.13	19.72	21.15
	5	21.17	24.61	26.10	29.87	23.36	26.56
0.09%	1	20.97	23.46	28.06	31.60	20.79	23.46
	2	22.38	24.02	25.52	28.63	19.59	23.70
	3	20.16	23.95	28.36	29.73	22.91	24.38
	4	20.89	24.28	23.20	26.99	20.94	22.98
	5	19.74	23.40	24.22	29.15	19.75	22.67
0.1%	1	21.45	24.12	27.93	30.13	20.08	24.27
	2	19.70	22.79	27.07	29.81	19.69	24.25
	3	21.91	23.60	26.91	31.55	18.35	21.03
	4	19.64	22.65	24.86	26.89	18.04	22.83
	5	20.32	23.87	25.38	28.83	17.77	20.87
0.2%	1	17.85	20.69	22.14	24.21	18.17	20.48
	2	17.60	20.37	20.96	23.45	15.56	19.74
	3	18.51	20.87	25.13	28.77	16.52	19.34
	4	16.88	20.42	24.56	28.24	15.42	18.70
	5	18.23	22.16	23.02	27.48	15.26	18.53
0.5%	1	17.30	19.46	21.46	24.90	16.85	18.08
	2	17.03	19.10	20.23	24.24	15.24	19.05
	3	16.26	18.99	19.09	22.70	16.21	18.34
	4	17.43	19.43	22.75	24.72	15.03	17.16
	5	16.18	19.08	22.88	24.09	17.70	19.04

Table 6. The simulation results, $PSNR_{seq}$ in dB, for the “Bream,” “Coastguard,” and “Weather” sequences, under different values of BER and N_{ave} , obtained using the proposed approach without/with the second (backtracking) procedure.

BER	N_{ave}	Bream		Coastguard		Weather	
		without	with	Without	with	without	with
0.01%	1	29.85	31.54	34.22	36.37	27.51	29.19
	2	30.54	31.36	30.10	33.15	30.81	31.53
	3	27.37	28.55	34.71	35.30	28.66	30.55
	4	26.71	27.21	34.36	35.84	30.86	32.77
	5	27.86	29.31	34.60	36.14	30.66	32.16
0.03%	1	24.75	25.98	32.11	33.26	26.06	27.35
	2	23.83	24.72	33.56	34.30	27.34	29.67
	3	25.88	26.63	33.71	34.76	24.73	26.07
	4	24.56	25.93	29.26	30.91	26.08	27.38
	5	24.89	25.59	31.20	32.14	27.49	28.45
0.05%	1	23.43	25.09	29.70	30.77	20.89	22.56
	2	24.39	25.40	30.77	32.84	21.83	23.17
	3	23.07	24.91	32.68	34.38	23.04	24.13
	4	25.53	26.16	31.15	33.05	24.57	25.55
	5	24.28	24.15	30.08	31.20	22.83	23.38
0.07%	1	21.91	23.30	29.53	30.90	25.31	26.71
	2	24.38	25.72	30.16	31.64	25.87	26.77
	3	21.12	22.53	24.65	27.82	25.87	26.95
	4	24.42	25.39	29.11	31.13	20.25	21.15
	5	23.78	24.61	28.48	29.87	25.88	26.56
0.09%	1	22.23	23.46	30.34	31.60	22.63	23.46
	2	22.98	24.02	26.98	28.63	22.11	23.70
	3	22.85	23.95	28.35	29.73	23.26	24.38
	4	23.61	24.28	25.65	26.99	21.56	22.98
	5	22.62	23.40	27.03	29.15	22.19	22.67
0.1%	1	22.43	24.12	28.88	30.13	23.56	24.27
	2	21.03	22.79	29.02	29.81	23.12	24.25
	3	22.39	23.60	29.63	31.55	19.79	21.03
	4	21.65	22.65	25.17	26.89	21.54	22.83
	5	22.54	23.87	27.89	28.83	19.62	20.87
0.2%	1	19.75	20.69	23.47	24.21	19.57	20.48
	2	18.14	20.37	22.34	23.45	18.14	19.74
	3	19.34	20.87	27.42	28.77	17.98	19.34
	4	18.70	20.42	26.78	28.24	17.88	18.70
	5	20.87	22.16	25.88	27.48	17.51	18.53
0.5%	1	18.35	19.46	22.67	24.90	17.42	18.08
	2	18.16	19.10	22.89	24.24	17.85	19.05
	3	17.58	18.99	21.59	22.70	16.99	18.34
	4	18.75	19.43	23.38	24.72	16.23	17.16
	5	17.73	19.08	22.80	24.09	17.89	19.04



Fig. 10. The simulation results obtained when the proposed detection and concealment approach is applied without (a) and with (b) the backtracking procedure to the first VOP of the “Weather” sequence with $BER = 0.05\%$ and $N_{ave} = 4$.

Based on the simulation results obtained in this study, several phenomena can be observed. (1) The smoother the original image, the better the corresponding error detection and concealment results. (2) The thresholds and weighting coefficients used in the proposed approach affect the performance of the proposed approach. (3) Based on the simulation results shown in Table 2 and Figs. 6-7, the corresponding concealment results for the proposed shape recovery approach indicate recovery of most of the shape data in P- and BVOPs. (4) Based on the simulation results shown in Tables 3-4 and Figs. 8-9, the concealment results obtained using the proposed approach are better than those obtained using the four existing error concealment approaches, namely, Zero-S, Spatial-M, Spectral-I, and Hybrid-A. (5) Based on the simulation results shown in Table 5, the concealment results obtained using the proposed hybrid cost function for texture error concealment $CF(C)$ are better than those obtained using the cost function $AIDB(C)$. (6) Based on the simulation results shown in Table 6 and Fig. 10, the concealment results obtained using the proposed error detection approach with two successive procedures are better than those obtained using the proposed error detection approach with the first procedure only.

Under the same BER and the same approach, the corresponding results for the corrupted images with larger N_{ave} are “usually” better than those for the corrupted images with smaller N_{ave} . That is, under the same BER (the same total number of error bits), on average, the case with larger N_{ave} will produce a smaller number of transmission errors than the case with smaller N_{ave} . However, in several situations, the above rule is invalid because the smaller number of transmission errors do not always produce a smaller number of corrupted blocks.

The proposed error detection approach can incorporate the channel coding strategy using error correcting codes. Some residual errors that remain in the received bitstream of the channel coding approach can be further detected and concealed using the proposed approach. Clearly, when the channel coding strategy is incorporated, the transmission bit rate will be moderately increased.

The proposed error concealment (postprocessing) approach can incorporate the error resilient (preprocessing) strategy. In fact, the proposed error concealment (postprocessing) approach can incorporate one or several error resilient (preprocessing) approach(es)

among the six categories, namely, the resynchronization approach, the robust entropy coding and prediction approach, the layer coding with unequal error protection approach, the multiple description coding approach, the data partitioning approach, and the RVLCs approach. The resynchronization approach has been embedded within several video compression standards, such as MPEG-1, MPEG-2, MPEG-4, H.261, and H.263 [1, 2, 8, 35, 36]. The data partitioning approach and the RVLCs approach can be optionally used in the MPEG-4 video compression standard [1, 2, 8, 13, 14]. As shown in Fig. 11, the data partitioning approach partitions a video packet into a shape and motion part and a texture part separated by a motion boundary marker (Fig.11 (a)) or into a shape part, a motion part, and a texture part separated by a shape marker and a motion marker (Fig.11 (b)). If the bitstream organization of Fig.11 (a) is employed, the data partitioning approach can achieve on average a performance gain of 2dB (with a 2~3% bit rate increment) over the wide range of test sequences and error conditions reported in [8, 13]. If a modified bitstream organization is employed, the data partitioning approach can achieve a performance gain of 0.2~1.2dB with a 4~6% bit rate increment as reported in [14]. On the other hand, RVLCs are special VLCs that have the prefix property when decoding is done in both the forward and reverse directions [8, 38, 39]. By using RVLCs, the decoder can recover some of the compressed data that would otherwise be discarded with a small loss of compression efficiency (with a 4.9~23% bit rate increment) [38]. In MPEG-4 [1], if only the texture data use RVLCs, a 1.5%~5% bit rate increment can be obtained [39]. RVLCs are useful when random byte errors occur, whereas RVLCs are not particularly helpful for IP transmission, where entire, relatively large packets are either received perfectly or not at all. As a summary, the proposed error concealment (postprocessing) approach can incorporate (without any difficulty) one or several error resilient (preprocessing) approaches among the six categories of error resilient strategies, and some performance gain can be obtained with some loss of compression efficiency (with a certain bit rate increment).

resync. marker	shape and motion data	motion boundary marker	texture data
-------------------	--------------------------	---------------------------	-----------------

(a) A video packet contains a shape and motion part and a texture part.

resync. marker	shape data	shape marker	motion data	motion marker	texture data
-------------------	---------------	-----------------	----------------	------------------	-----------------

(b) A video packet contains a shape part, a motion part, and a texture part.

Fig. 11. Bitstream organization of an MPEG-4 data partitioning video packet.

The proposed error detection and concealment (postprocessing) approach is particularly applicable when random or a burst error occur, i.e., in a wireless transmission channel, and is not particularly helpful for IP transmission, where entire, relatively large packets are either received perfectly or not at all. The proposed approach is applicable under a wide range of transmission bit rates (20k~1M Hz). Based on the experimental

results obtained in this study, the proposed approach can recover high-quality MPEG-4 images from the corresponding corrupted MPEG-4 images up to a bit error rate (BER) of 0.5%.

The computational time required by the first procedure (checking a set of error-checking conditions) of the proposed error detection approach is almost constant. The second procedure (a backtracking procedure) of the proposed error detection approach is enabled only when an error is detected by the first procedure of the proposed error detection approach. Therefore, the computational time required by the second procedure of the proposed error detection approach is approximately proportional to the number of detected errors. On the other hand, the computational time required by the proposed error concealment approach (both shape and texture) is approximately proportional to the corresponding number of corrupted blocks. Based on the simulation results obtained in this study, if a 2.4 GHz PC is employed, the proposed error detection procedure can be operated in real-time, and the proposed error detection and concealment (postprocessing) approach can be operated in near-real-time (about 20 video frames/sec) when the bit error rate = 0.1%.

4. CONCLUDING REMARKS

In this study, a postprocessing approach to detection and concealment of transmission errors in MPEG-4 images has been proposed. In the proposed approach, transmission errors within a video packet are detected by means of two successive procedures: (1) whether the video packet is corrupted or not is determined by checking a set of error-checking conditions, and then (2) the precise location (block-based) of the first transmission error within the corrupted video packet is verified by using a backtracking procedure. To recover the corrupted shape data, the shape error concealment approach to intra-coded IVOPs proposed in [4] is adopted, and a shape error concealment approach to inter-coded P- and BVOPs has been proposed in this study. To recover corrupted texture data, several existing and proposed concealment techniques are employed together to generate a set of possible concealment candidates for a corrupted texture block. Then, a proposed objective cost function for texture error concealment is used to determine the "best" texture error concealment candidate among the set of generated candidates as the concealed texture block for the corrupted texture block. Based on the simulation results obtained, the proposed approach can recover high-quality MPEG-4 images from the corresponding corrupted MPEG images without increasing the transmission bit rate. This shows the feasibility of the proposed approach.

REFERENCES

1. ISO/IEC JTC1/SC29/WG11 N3093, *MPEG-4 Video Verification Model Version 15.0*, 1999.
2. Y. Wang and Q. F. Zhu, "Error control and concealment for video communication: a review," in *Proceedings of the IEEE*, Vol. 86, 1998, pp. 974-997.
3. M. R. Frater, W. S. Lee, M. Pickering, and J. F. Arnold, "Error concealment in video

- coding of arbitrarily shaped objects,” *Signal Processing: Image Communications*, Vol. 15, 2000, pp. 631-641.
4. S. Shirani, B. Erol, and F. Kossentini, “A concealment method for shape information in MPEG-4 coded video sequences,” *IEEE Transactions on Multimedia*, Vol. 2, 2000, pp. 185-190.
 5. P. J. Lee, L. G. Chen, W. J. Wang, and M. J. Chen, “Robust error concealment algorithm for MPEG-4 with the aids of fuzzy theory,” in *IEEE International Conference on Consumer Electronics*, 2001, pp. 154-155.
 6. A. Poli and L. Huguet, *Error Correcting Codes*, Englewood Cliffs, New Jersey: Prentice Hall, 1992.
 7. H. Ohta and T. Kitami, “A cell loss recovery method using FEC in ATM networks,” *IEEE Journal on Selected Areas in Communications*, Vol. 9, 1991, pp. 1471-1483.
 8. R. Talluri, “Error-resilient video coding in the ISO MPEG-4 standard,” *IEEE Communications Magazine*, Vol. 36, 1998, pp. 112-119.
 9. D. W. Redmill and N. G. Kingsbury, “The EREC: an error-resilient technique for coding variable-length blocks of data,” *IEEE Transactions on Image Processing*, Vol. 5, 1996, pp. 565-574.
 10. P. Frossard and O. Verscheure, “AMISP: a complete content-based MPEG-2 error-resilient scheme,” *IEEE Transactions on Circuits and Systems for Video Technology*, Vol. 11, 2001, pp. 989-998.
 11. M. Gallant and F. Kossentini, “Rate-distortion optimized layered coding with unequal error protection for robust internet video,” *IEEE Transactions on Circuits and Systems for Video Technology*, Vol. 11, 2001, pp. 357-372.
 12. Y. Wang and S. Lin, “Error-resilient video coding using multiple description motion compensation,” *IEEE Transactions on Circuits and Systems for Video Technology*, Vol. 12, 2002, pp. 438-452.
 13. R. Talluri, I. Moccagatta, Y. Nag, and G. Cheung, “Error concealment by data partitioning,” *Signal Processing: Image Communications*, Vol. 14, 1999, pp. 505-518.
 14. K. C. Roh, K. D. Seo, and J. K. Kim, “Data partitioning and coding of DCT coefficients based on requantization for error-resilient transmission of video,” *Signal Processing: Image Communications*, Vol. 17, 2002, pp. 573-585.
 15. T. Stockhammer, H. Jenkac, and C. Weiß, “Feedback and error protection strategies for wireless progressive video transmission,” *IEEE Transactions on Circuits and Systems for Video Technology*, Vol. 12, 2002, pp. 465-482.
 16. W. L. Shyu and J. J. Leou, “Detection and correction of transmission errors in facsimile images,” *IEEE Transactions on Communications*, Vol. 44, 1996, pp. 938-948.
 17. Y. H. Han and J. J. Leou, “Detection and correction of transmission errors in JPEG images,” *IEEE Transactions on Circuits and Systems for Video Technology*, Vol. 8, 1998, pp. 221-231.
 18. X. Lee, Y. Q. Zhang, and A. Leon-Garcia, “Information loss recovery for block-based image coding techniques – a fuzzy logic approach,” *IEEE Transactions on Image Processing*, Vol. 4, 1995, pp. 259-273.
 19. Y. Wang, Q. F. Zhu, and L. Shaw, “Maximally smooth image recovery in transform coding,” *IEEE Transactions on Communications*, Vol. 41, 1993, pp. 1544-1551.
 20. J. W. Kim, J. W. Park, and S. U. Lee, “DCT coefficients recovery-based error concealment technique and its application to the MPEG-2 bit stream error,” *IEEE*

- Transactions on Circuits and Systems for Video Technology*, Vol. 7, 1997, pp. 845-854.
21. H. Sun and W. Kwok, "Concealment of damaged block transform coded images using projections onto convex sets," *IEEE Transactions on Image Processing*, Vol. 4, 1995, pp. 470-477.
 22. W. Kwok and H. Sun, "Multi-directional interpolation for spatial error concealment," *IEEE Transactions on Consumer Electronics*, Vol. 39, 1993, pp. 455-460.
 23. S. S. Hemami and T. H. Y. Meng, "Transform coded image reconstruction exploiting interblock correlation," *IEEE Transactions on Image Processing*, Vol. 4, 1995, pp. 1023-1027.
 24. Z. Wang, Y. Yu, and D. Zhang, "Best neighborhood matching: an information loss restoration technique for block-based image coding systems," *IEEE Transactions on Image Processing*, Vol. 7, 1998, pp. 1056-1061.
 25. J. W. Suh and Y. S. Ho, "Error concealment based on directional interpolation," *IEEE Transactions on Consumer Electronics*, Vol. 43, 1997, pp. 295-302.
 26. P. J. Lee and M. J. Chen, "Robust error concealment algorithm for video decoder," *IEEE Transactions on Consumer Electronics*, Vol. 45, 1999, pp. 851-859.
 27. M. Ghanbari and V. Seferidis, "Cell-loss concealment in ATM video codecs," *IEEE Transactions on Circuits and Systems for Video Technology*, Vol. 3, 1993, pp. 238-247.
 28. M. Wada, "Selective recovery of video packet loss using error concealment," *IEEE Journal on Selected Areas in Communications*, Vol. 7, 1989, pp. 807-814.
 29. J. Feng, K. T. Lo, and H. Mehrpour, "Error concealment for MPEG video transmissions," *IEEE Transactions on Consumer Electronics*, Vol. 43, 1997, pp. 183-187.
 30. L. H. Kieu and K. N. Ngan, "Cell-loss concealment techniques for layered video codes in an ATM network," *IEEE Transactions on Image Processing*, Vol. 3, 1994, pp. 666-677.
 31. F. Zhu, Y. Wang, and L. Shaw, "Coding and cell-loss recovery in DCT-based packet video," *IEEE Transactions on Circuits and Systems for Video Technology*, Vol. 3, 1993, pp. 248-258.
 32. H. Sun, K. Challapalli, and J. Zdepski, "Error concealment in digital simulcast AD-HDTV decoder," *IEEE Transactions on Consumer Electronics*, Vol. 38, 1992, pp. 108-118.
 33. W. Keck, "A method for robust decoding of erroneous MPEG-2 video bitstreams," *IEEE Transactions on Consumer Electronics*, Vol. 42, 1996, pp. 411-421.
 34. P. Cuenca, L. Orozco-Barbosa, A. Garrido, F. Quiles, and T. Olivares, "A survey of error concealment schemes for MPEG-2 video communications over ATM networks," in *Proceedings of Canadian Conference on Electrical and Computer Engineering*, 1997, pp. 118-121.
 35. W. J. Chu and J. J. Leou, "Detection and concealment of transmission errors in H.261 images," *IEEE Transactions on Circuits and Systems for Video Technology*, Vol. 8, 1998, pp. 74-84.
 36. H. C. Shyu and J. J. Leou, "Detection and concealment of transmission errors in MPEG-2 images – a genetic algorithm approach," *IEEE Transactions on Circuits and Systems for Video Technology*, Vol. 9, 1999, pp. 937-948.
 37. J. W. Kim, J. W. Park, and S. U. Lee, "Error-resilient decoding of randomly impaired

- MPEG-2 bit stream,” in *Proceedings of SPIE*, Vol. 2227, 1996, pp. 78-88.
38. Y. Takishima, M. Wada, and H. Murakami, “Reversible variable length codes,” *IEEE Transactions on Communications*, Vol. 43, 1995, pp. 158-162.
39. J. Wen and J. D. Villasenor, “A class of reversible variable length codes for robust image and video coding,” in *Proceedings of IEEE International Conference on Image Processing*, 1997, pp. 65-68.



Chien-Ming Lee (李健銘) was born in I-Lan, Taiwan, R.O.C. on August 13, 1977. He received the B.S. degree in Computer Science and Information Engineering in 1999 from Fu Jen Catholic University, Taipei, Taiwan and the M.S. degree in Computer Science and Information Engineering in 2001 from National Chung Cheng University, Chiayi, Taiwan. His current research interests include image processing, pattern recognition, and computer vision.



Jin-Jang Leou (柳金章) was born in Chiayi, Taiwan, R.O.C. on October 25, 1956. He received the B.S. degree in Communication Engineering in 1979, the M.S. degree in Communication Engineering in 1981, and the Ph.D. degree in Electronics in 1989, all from National Chiao Tung University, Hsinchu, Taiwan. From 1981 to 1983, he served in the Chinese Army as a Communication Officer. From 1989, he has been on the faculty of the Department of Computer Science and Information Engineering at National Chung Cheng University, Chiayi, Taiwan. His current research interests include image/video processing, image/video communication, pattern recognition, and computer vision.